Structural Features of the Aβ Amyloid Fibril Elucidated by Limited Proteolysis[†]

Indu Kheterpal, Angela Williams, Charles Murphy, Brian Bledsoe, and Ronald Wetzel*

Graduate School of Medicine, University of Tennessee Medical Center,1924 Alcoa Highway, Knoxville, Tennessee 37920

Received April 19, 2001; Revised Manuscript Received July 6, 2001

ABSTRACT: Although the gross morphology of amyloid fibrils is fairly well understood, very little is known about how the constituent polypeptides fold within the amyloid folding motif. In the experiments reported here, we used trypsin and chymotrypsin to conduct limited proteolysis studies on synthetic amyloid fibrils composed of the Alzheimer's disease peptide Aβ(1−40). In both reactions, the extreme N-terminal proteolytic fragment is released from fibrils as rapidly as it is from the Aβ monomer, while other proteolytic fragments are generated much more slowly. Furthermore, aggregated material isolated by centrifugation of intermediate digestion time points from both proteases contains, in addition to full-length material, peptides that possess mature C-termini but truncated N-termini. These data strongly suggest that the N-terminal region of Aβ is not involved in the β-sheet network of the amyloid fibril, while the C-terminus is essentially completely engaged in protective—presumably β-sheet—structure. In both digests, release of the extreme N-terminal fragments of Aβ(1−40) reaches plateau values corresponding to about 80% of the total available Aβ. This suggests that there are two classes of peptides in the fibril: while the majority of Aβ molecules have an exposed N-terminus, about 20% of the peptides have an N-terminus that is protected from proteolysis within the fibril structure. The most likely cause of this heterogeneity is the lateral association of protofilaments into the fibril structure, which would be expected to generate a unique environment for those Aβ N-termini located at protofilament packing interfaces and/or in the interior core region between the packed protofilaments. This suggests that the N-terminal region of Aβ, while not directly involved in the β-sheet network of the fibril, may contribute to fibril stability by participating in protofilament packing.

There are over 15 human disease states now known to be associated with amyloid fibrils or their assembly intermediates (*1*−*3*). Despite a lack of significant sequence homology between the constituent proteins, amyloid fibrils appear to share common structures, as evidenced by very similar fibrillar morphologies (*1*) and X-ray diffraction patterns indicative of cross-β-sheet structure (*4*). Very little is known, however, about how the constituent proteins thread into this apparent common folding motif. Since the available methods of high-resolution structure determination are not capable of addressing the structures of these large, polydisperse, insoluble aggregates, structural information at lower resolution has become increasingly important. Recently, we used hydrogen−deuterium exchange to show that only about 50% of the 39 backbone amide protons in the Aβ peptide associated with Alzheimer's disease plaques are protected from exchange when the peptide is incorporated into amyloid fibrils. This suggests that a significant portion of this relatively short sequence is in fact not involved in the protective H-bonded structure (*5*). Such data immediately introduce the questions of which portions of the peptide sequence are exposed to exchange and which are involved in β-sheet structure.

An intermediate resolution technique that has been used in structural analysis of globular proteins is limited proteolysis (*6*−*8*). Protease binding sites typically require the availability of up to 10 amino acid residues in an accessible, flexible conformation (*8*). If a globular protein undergoes a single proteolytic cleavage event at a particular site under controlled, partial proteolysis conditions, it can be concluded that this site must be in an exposed, flexible, or weakly structured portion of the protein in the native state (*8*). The technique is particularly effective in dissecting multidomain structure within proteins (*6*), but it has also been used to characterize native oligomeric protein structure (*6*) as well as partially folded intermediates and flexible sites within proteins (*7*). Although, in principle, it should be possible to probe the structure of insoluble protein aggregates by such a limited proteolysis analysis, certain technical limitations, such as inefficient mixing, might be expected to thwart this approach. We show here, however, that limited proteolysis can provide valuable structural information on amyloid fibrils. Consistent with previous hydrogen−deuterium exchange analysis (*5*), our data suggest that some segments of the Aβ(1−40) sequence are not involved in the protective β-sheet in the fibril structure. In particular, the hydrophilic, N-terminal portion of this peptide is exposed to proteolytic cleavage under native conditions.

MATERIALS AND METHODS

Fibril Synthesis. Aβ fibrils were grown from chemically synthesized Aβ(1−40) peptide (Keck Biotechnology Center,

[†] Supported in part by the Lindsay Young Alzheimer's Disease Research Gift Fund, the Reuben Louise Cates Mount Research Endowment, an Alzheimer's Association Zenith Award to R.W., and an NIH individual national research service award (F32 AG05869) to I.K.

* To whom correspondence should be addressed.

10.1021/bi010805z CCC: $20.00
Published on Web 09/08/2001

Yale University) disaggregated by a TFA/HFIP[1] protocol as described previously (*5*). Briefly, Aβ peptide was treated with TFA (Pierce) and HFIP (Acros) to remove any preexisting aggregates (*9*). The disaggregated peptide was then dissolved stepwise in equal volumes of 2 mM NaOH and 2× PBS, pH 7.4, containing 0.1% sodium azide to give a peptide concentration of approximately 50 μM and then ultracentrifuged for 18 h at 50000*g* to remove any remaining aggregates. The fibril formation reaction was initiated by addition of a small quantity of preformed sonicated Aβ(1−40) fibrils at a weight ratio of 1:750 and incubation at 37 °C in PBS, pH 7.4. Fibril growth was monitored using thioflavin assay (*10*) until complete (~7 days).

Besides amyloid fibrils, Aβ(1−40) can form at least one additional type of aggregate (*11*) as well as several assembly intermediates on the way to fibrils (*12*). Fibrils grown in vitro may be of variable quality depending on details of the growth conditions and perhaps also on the purity of the starting peptide. It is clearly critical that the aggregates used for structural studies be highly enriched in the object of interest—in the case of this paper, the final amyloid fibril product. Different aggregate types can be characterized by electron microscopy (*11*), but this is not a quantitative method for assessing the bulk quality of a product. As described previously (*5*), we prepare fibrils from rigorously disaggregated monomer solutions seeded with sonicated fibrils grown previously. Seeding with past batches of fibrils ensures historical consistency of the fibril product and may also promote a degree of quality—at least to the extent that the seed fibrils are themselves of good quality. Characterization of the fibril product may be as important as the means by which it is made. Besides EM, we compare new batches of fibrils for structural studies to older batches made in our laboratory in terms of the thioflavin T signals per weight of fibril. The kinetics of hydrogen−deuterium exchange (*5*) may prove to be an especially discriminating measure of fibril quality.

Proteolysis Conditions. The disaggregated Aβ monomer[2] and Aβ fibrils were subjected to proteolysis using trypsin (Promega) and α-chymotrypsin (Sigma) at a weight ratio of 1:10 (enzyme to protein) for all of the experiments presented here. At this enzyme ratio the Aβ monomer was determined to be completely digested, as evidenced by the disappearance of the HPLC peak for the monomer, within 25 min using trypsin and 120 min using chymotrypsin.

For trypsin digestion of the monomer, the Aβ monomer was dissolved at 87 μM in 50 mM Tris-HCl buffer (pH 7.6) containing an appropriate concentration of freshly added trypsin. Aliquots of this mixture were removed in triplicate after various time intervals as shown in Figure 3. Several time zero aliquots were removed prior to the addition of trypsin to be used later to determine, by HPLC analysis, the total amount of peptide in a digest aliquot. All of the reactions were stopped by diluting the reaction mixture with 1% aqueous TFA to a final Aβ concentration of 19 μM. This mixture had previously been determined to quickly dissolve Aβ fibrils, inactivate the protease, and in addition suppress amyloid formation by Aβ in autosampler vials during long programmed HPLC analytical runs. A 60 min time point of a monomer digest was chromatographed by HPLC, and the collected peaks were analyzed by electrospray ionization mass spectrometry (ESI-MS) and, in some cases, by amino acid sequence analysis.

For trypsin digestion of fibrils, Aβ fibrils were collected by centrifugation, washed once with the Tris reaction buffer, and then resuspended in Tris buffer plus trypsin to give a weight concentration of fibrils equivalent to 87 μM Aβ monomer. Aliquots were removed in triplicate at time intervals shown in Figure 3. One set of aliquots was removed before the addition of trypsin to establish by HPLC analysis the exact amount of Aβ in the aliquot. All reactions were stopped by diluting Aβ to 19 μM with 1% aqueous TFA and reaction mixtures analyzed using HPLC. A 30 min digest of fibrils was quenched with 1% aqueous TFA, and the HPLC fractions were subjected to ESI-MS and sequence analysis to identify breakdown products.

Digestion of the monomer and fibrils by chymotrypsin was the same as described above for trypsin except that the digestion buffer was 80 mM Tris-HCl, pH 7.9. HPLC separation of digestion products for MS and amino acid sequencing analysis of fragments was conducted using a 180 min time point for the monomer and a 180 min time point for fibrils. Kinetic time points were analyzed as shown in Figure 5.

HPLC Conditions. Peptide digests were separated using a high-performance liquid chromatography series 1100 quaternary pump system (Hewlett-Packard, HP) with a 3 × 150 mm C3 column (HP) containing Zorbax stable bond packing. The solvent flow rate was 1 mL/min, and the temperature was controlled at 25 °C. Solvent A was 0.05% TFA in HPLC-grade water (Fisher), and solvent B was 0.05% TFA in HPLC-grade acetonitrile (Fisher). Samples were injected into the column equilibrated to 1% solvent B and eluted with a linear gradient of 1%−51% solvent B over a 25 min period. The separation was monitored by absorbance at 215 nm.

ESI-MS. A PE-SCIEX Type 150 EX (Perkin-Elmer) single quadrupole electrospray ionization mass spectrometer (ESI-MS) was used to identify peptide fragments isolated by prep collection from HPLC. The collected fractions after chromatography were dried down in a vacuum centrifuge, redissolved in 20% acetonitrile and 0.5% TFA, and infused into MS at a flow rate of 5 μL/min using a Harvard Apparatus Model 11 syringe pump. Experiments were performed in the positive ion mode with a capillary voltage of 4.8 kV, alternating mode orifice voltage of 31 V, and a ring voltage of 230 V. The source temperature was maintained at 25 °C. All spectra were acquired in the multichannel accumulation mode over a mass range of 200−2150 Da at 333 Da/s. Spectra were analyzed using the Biomultiview program provided by the system manufacturer (PE-SCIEX, Perkin-Elmer).

Sequence Analysis. For N-terminal sequencing, HPLC fractions were dried down to 10 μL and placed in the glass fiber blot cartridge of an ABI model 494 Procise automated amino acid sequencer (Perkin-Elmer). The N-terminal amino

[1] Abbreviations: PBS, phosphate-buffered saline; Tris, tris(hydroxymethyl)aminomethane; HPLC, high-performance liquid chromatography; TFA, trifluoroacetic acid; HFIP, 1,1,1,3,3,3-hexafluoro-2-propanol; ESI-MS, electrospray ionization mass spectrometry; AD, Alzheimer's disease; APP, β amyloid precursor protein.

[2] There is at present a lack of experimental agreement as to whether fully disaggregated Aβ in native aqueous buffer is a monomer or dimer. Throughout this paper we use the word monomer to refer to the predominant low molecular weight form of Aβ in PBS.

acid sequence was determined using the pulsed-liquid cycle as per the manufacturer's directions.

Quantitation of Peptides from Protease Digests. To compare the rates of proteolytic generation of different peptide fragments from both the monomer and fibrils, we had to calculate the mole fraction, with respect to moles of starting Aβ, of each peptide generated. To obtain the moles of peptide fragments in HPLC, we determined a factor relating the weight amount of Aβ(1−40) injected onto the HPLC to the A_{215} area of the resulting peak. For our HPLC system and detector, this value was found to be 1218 area units/μg. Since absorbance by Aβ at A_{215} is primarily attributable to the peptide bond, and since the weight of the peptide increases roughly in proportion to the number of peptide bonds, we made the working assumption that this value could also be used to calculate the *weights* of Aβ fragments from their HPLC peak areas at A_{215}. [This is clearly an approximation and will be inexact due to the different molecular weights of peptide fragments of equivalent lengths, the nonlinearity of the peptide weight to peptide bond number as fragment size decreases, and the possibility that more hydrophobic peptides may not chromatograph efficiently. However, as seen below, the approximation works remarkably well for most of the fragments and, under ideal cases, can also be corrected by normalization.]

For each peptide peak at each time point, peak areas were converted to micrograms as above and then converted to moles using the molecular weight of the identified fragment. The number of moles of fragment was divided by moles of starting peptide in the digest to give the mole fraction recovery at each time. In cases where the cleavage reaction clearly goes to completion (for example, the release of the 1−4 fragment from the monomer, as shown in Figure 5A), the mole fraction at the plateau value is often very close to the expected value of 1.0 using the approximation described above. In cases where the kinetics of peptide release for the completely digested monomer reached a plateau at a value other than 1.0 (presumably because of one or more of the factors described above), we normalized all of the data points of both the monomer and fibril curves by the factor necessary to bring the monomer curve to the theoretically expected value of 1.0 (for example, see Figure 3A). It can be seen from Figure 3 that these adjustments were generally small. Furthermore, we obtained independent results for the major trypsin fragments, using the double digest method described in the Results section, that strongly validate the approach for quantifying the fibril digestion kinetics described above.

RESULTS

To establish the identities and chromatographic properties of proteolytic fragments, we exposed Aβ(1−40) monomers to proteolysis by trypsin and chymotrypsin under conditions identical to those used in subsequent fibril digestion experiments. Figure 1 shows the HPLC elution profiles of the complete trypsin (60 min) and chymotrypsin (180 min) digestion reactions. As discussed below, digestion reactions of fibrils also produce some additional peptides that contain potential cleavage sites that are apparently protected within the core structure of the digested aggregate. With a few minor exceptions,[3] Table 1 lists all of the peptides observed in these studies, as characterized by the retention times of the HPLC

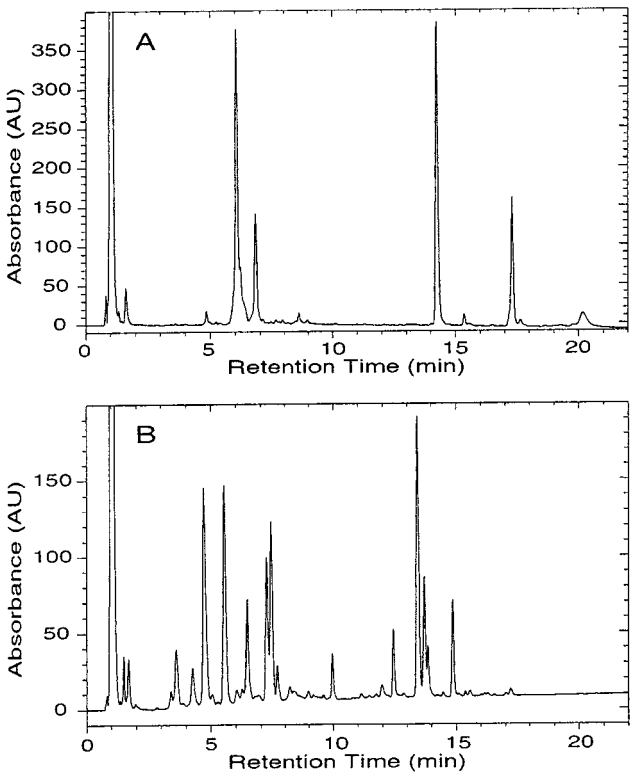

FIGURE 1: HPLC profiles of the Aβ monomer completely digested with (A) trypsin and (B) chymotrypsin. The peptide and protease ratio is 10:1 by weight. The digestion using trypsin was carried out for 60 min, and the digestion using chymotrypsin was carried out for 180 min. All of the peaks were collected after HPLC and identified using ESI-MS and/or amino acid sequence analysis.

peaks and identified by mass spectrometry and/or amino acid sequencing. Figure 2 summarizes the peptides obtained in various trypsin and chymotrypsin digests of Aβ(1−40).

Amyloid fibril formation reactions can reach equilibrium positions significantly short of complete aggregation, depending on buffer conditions and peptide sequence and concentration (*13*). To minimize the complicating impact of the presence of monomeric Aβ in fibrils subjected to limited proteolysis analysis, we isolated the fibrils by centrifugation and resuspended them in buffer, immediately before the start of the proteolysis reaction. Despite these efforts, it is likely—as discussed below—that some monomer dissociates from fibrils and is rapidly digested, during the proteolysis of fibrils. Because such monomer digestion products complicate the data and bias the interpretation of the results, we attempted to minimize the proteolysis reaction time by using a relatively large amount of protease in the digests. We expect that by enhancing the proteolysis rate for fibrils with the aid of high protease levels, digestion times—and therefore the time available for fibril dissociation—will be minimized.

Trypsin Reactions. Figure 3 shows time courses for the generation of trypsin fragments from the Aβ(1−40) monomer and fibrils at pH 7.6 and 25 °C. Each panel compares the kinetics of generation of a single fragment from the monomer vs the fibril. As discussed later, other fragments are generated besides those shown in Figure 2, but these could not be

[3] The exceptions are a few transient proteolysis intermediates observed in the chymotrypsin digest of Aβ fibrils and one fragment, the 17−40, observed in the trypsin digest of the Aβ monomer.

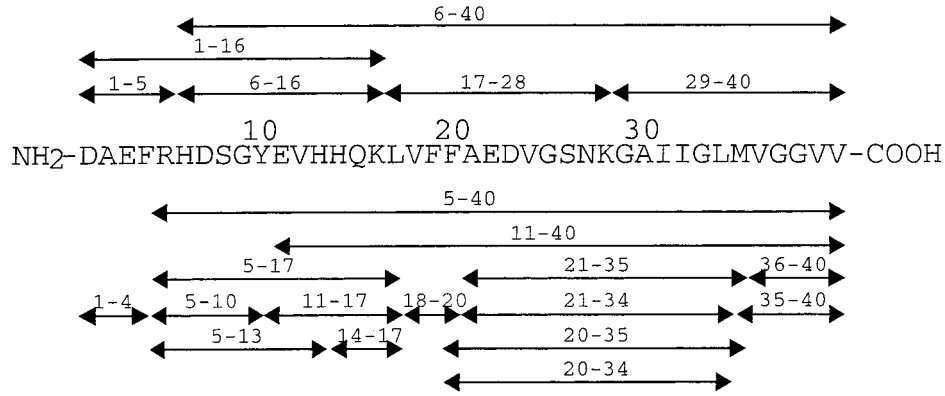

FIGURE 2: Amino acid sequence of Aβ(1−40). Shown schematically above the sequence are the fragments identified from the trypsin digestions. Shown schematically below the sequence are the corresponding chymotrypsin fragments.

Table 1: Fragments Obtained from Proteolytic Digests of Aβ[a]

fragment	retention time (min)	calculated mass (Da)	measured mass (Da)
trypsin			
6−16	6.05	1336.39	1336.30
1−5	6.80	636.66	636.60
1−16	8.63	1955.03	1955.00
17−28	14.23	1325.48	1325.20
1−40, 6−40, 29−40	17.31	4329.86, 3711.22, 1085.38	4329.70, 3711.30, 1085.30
chymotrypsin			
14−17	3.60	524.40	524.6
unidentified	4.26		
5−10	4.71	733.74	733.40
11−17	5.54	890.01	889.90
5−13	6.46	1099.01	1099.1
36−40	7.23	429.5	429.27
1−4	7.42	480.47	480.30
unidentified	7.67		
5−17	8.38	1605.73	1605.46
35−40	9.96	560.72	560.40
21−34	12.45	1343.20	1343.10
18−20	13.42	411.50	411.30
21−35	13.70	1474.70	1474.5
20−34	13.86	1490.2	1490.6
20−35	14.87	1621.88	1621.58
5−40	17.12	3867.41	3866.8
1−40	17.29	4329.86	4329.7
11−40	17.59	3151.6	3151.4

[a] As described in Materials and Methods, Aβ(1−40) fibrils were digested with protease and HPLC chromatographed, and the collected peaks were identified by mass spectrometry, with N-terminal sequence analysis used to confirm peaks with ambiguous MS fragment patterns.

quantified in our HPLC system due to overlapping retention times (see Table 1). Since kinetics were conducted by quenching representative aliquots of the fibril digest, the data represent the amount of each peptide present whether it was released into solution or remained (noncovalently) associated with the fibril. Data are presented as the mole fraction of each peptide with respect to the moles of Aβ(1−40) present in a comparable aliquot at $t = 0$. Moles of peptide were calculated as described in Materials and Methods.

Panels A (6−16 fragment), B (1−5 fragment), and D (17−28 fragment) immediately suggest that the trypsin digestion of the monomer under these conditions is essentially over after about 25 min, since the mole fraction of peptide released from monomer reaches a maximum for all three of these peptides at about 25 min. Panel C shows the progress curve for generation of the 1−16 peptide. In the digest of the monomer, this peptide is generated very rapidly to a mole fraction of about 0.6, after which it decays, finally essentially disappearing at 25 min. This behavior is clearly because it is a reaction intermediate, containing a viable trypsin site at residue 5 (see Figure 2).

As discussed in Materials and Methods, the use of the μg/A_{215} conversion factor derived from Aβ(1−40) for all peptide fragments is an approximation. It is therefore somewhat surprising that the conversion works so well in generating the data shown for the monomer digests in Figure 3. The progress curves for the 6−16 (Figure 3A), 1−5 (Figure 3B), and 17−28 (Figure 3D) fragments reach maximum mole fraction values of about 1.10, 0.85, and 0.95, respectively, very close to the expected value of 1.0. To more accurately interpret the fibril digests, we normalized both the monomer and fibril data in panels A, B, and D by factors necessary to bring the monomer digest curves to the theoretical maximum mole fraction of 1.0. The underlying assumption in making this normalization is that there should be no impediments to the monomer digest going to completion. The data in panel C cannot be so normalized, since, as a reaction intermediate that disappears from the complete digest, there is no basis for which to conduct the normalization; this curve thus remains only an approximation.

In contrast to the monomer digestion reactions, most of the proteolytic fragments are generated very slowly in the fibril digests. Fragment 17−28 (Figure 3D) accumulates to (normalized) mole fractions of about 0.22 at 30 min and 0.29 at 60 min, while fragment 6−16 (Figure 3A) accumulates to mole fractions of about 0.28 at 30 min and 0.35 at 60 min. Furthermore, essentially no 1−16 fragment (Figure 3C) is observed throughout the fibril digest. There are at least two reasonable interpretations of the relatively slow, but finite, release of these fragments in the fibril digests. It is possible that the relevant cleavage sites are in the relatively weak structure within the fibril and that cleavage occurs only when the cleavage site becomes transiently available through thermal motion within the fibril. Alternatively, it is possible that these bonds are unavailable in the fibril structure and that generation of the peptide fragments occurs through a slow release from the fibril of either Aβ(1−40) itself and/or its partial proteolysis fragments, followed by a relatively rapid trypsin digestion of the released peptides. This latter explanation is supported by the very similar progress curves observed, for example, for release of the 17−28 and 6−16 fragments. The ambiguity surrounding generation of these fragments, plus the general difficulty in inferring structural

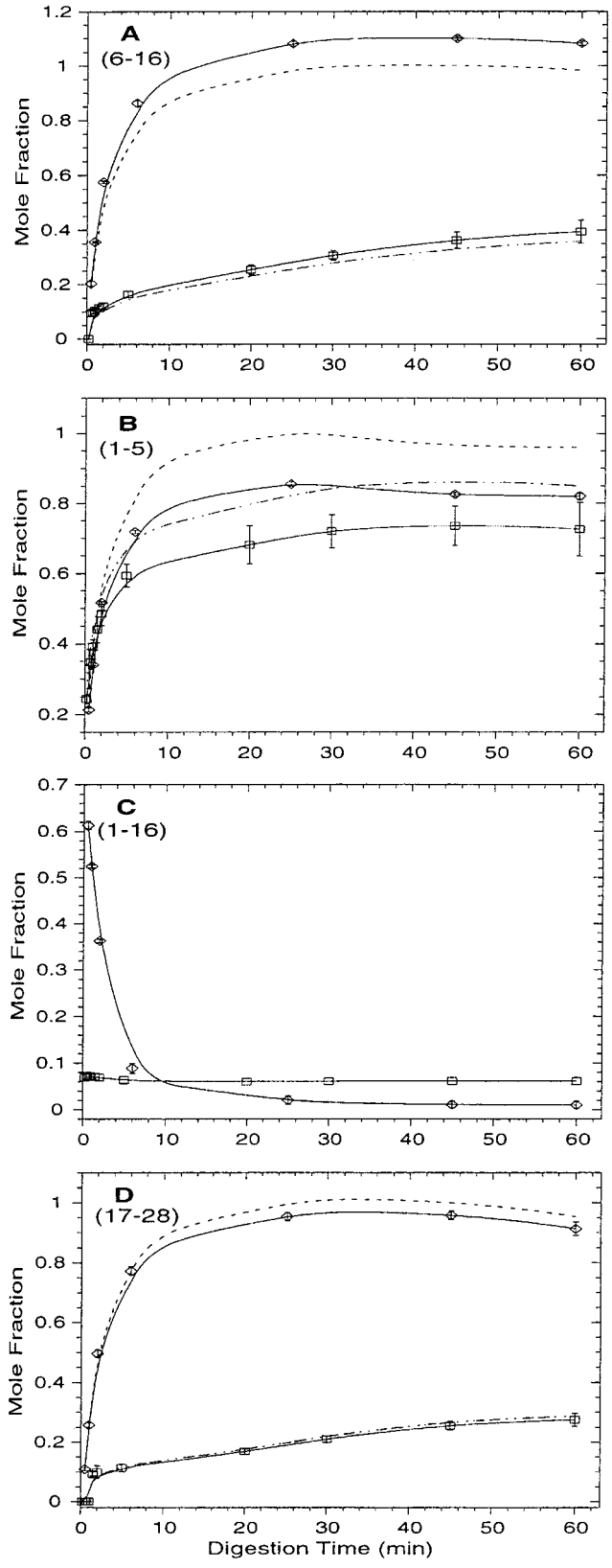

FIGURE 3: Mole fraction of peptides released after tryptic digestion vs time from the monomer (◇) and fibrils (□). The data points have been connected by a smoothing algorithm. Standard deviations shown are from triplicate analysis. The mole fraction of each peptide released was calculated and normalized as described in the text, and the normalized curves for the monomer (---) and fibrils (•• – ••) are also presented. The 1−16 peptide is an intermediate and was not normalized.

information from *secondary* cleavages in limited proteolysis reactions of proteins, makes more detailed interpretation of the data for the 6−16 and 17−28 fragments difficult.

However, interpretation of the release of the 1−5 fragment is relatively straightforward. This fragment is released rapidly in the fibril digest, exhibiting essentially the same initial rate of release as for the monomeric peptide (Figure 3B). The rapid release of the 1−5 fragment suggests that the 5−6 peptide bond of Aβ(1−40), as well as the flanking 2−5 amino acids upstream and downstream (*8*), is as mobile and unrestricted in the fibril as it is in the monomer. This speaks against the involvement of the N-terminal 7−8 residues in the stable β-sheet structure in the fibril.

Despite the rapid release of the 1−5 peptide, the kinetics of 1−5 fragment generation reaches a plateau at a (normalized) mole fraction of about 0.80, after which essentially no more 1−5 fragment is released. Because of the potential importance of this result, it is critical to rule out trivial explanations and to confirm this result independently. First, it is clear that incomplete release of the 1−5 peptide is not a consequence of inactivation of trypsin during the cleavage reaction. This is shown in Figure 3 by the ongoing release curves for other peptides even while 1−5 release (within the same proteolysis reaction) has reached a plateau. Another possible explanation for a plateau at less than a 1.0 mole fraction is a technical limitation on complete recovery of the peptide during analysis of the fibril digests. To exclude this possibility, we designed two independent experiments to demonstrate that incomplete recovery of 1−5 is because of incomplete proteolytic cleavage of the Arg_5−His_6 bond, as described next.

In the first approach, we generated two sets (of triplet repeats) of 60 min trypsin digestion reactions of fibrils. The first set was worked up in the normal manner (solubilized and analyzed by HPLC) to generate peak areas of the 1−5 peptide released from the fibrils. The second set of digests was processed in 100% TFA to completely dissolve and disaggregate any fibrillar material remaining in the 60 min digest time point. This material was then dried down, dissolved in trypsin reaction buffer, and redigested with trypsin. These replicate time points were then chromatographed and the 1−5 peptides quantified. The mean value for 1−5 peptide released in the single trypsin digest was 814 ± 8 area units, while the value for the double digest (1−5 originally released, plus 1−5 released after residual fibrillar material was resolubilized to monomer) was 1032 ± 62 area units. This experiment shows that only 80% of the total available 1−5 peptide is obtained at the plateau point in the original trypsin digest of fibrils, in agreement with the normalized data shown in Figure 3B. [Comparable "double digest" analysis showed that the 17−28 fragment obtained after 60 min of fibril digestion represented 31% of the total available peptide and that the 6−16 fragment represented 35% of the total available peptide; these numbers are in excellent agreement with the mole fractions (0.29 and 0.35) calculated from the normalized digest analysis shown in Figure 3 and described above. Together, these data suggest that the kinetic data shown in Figure 3 are not significantly disturbed by differences in chromatographic efficiencies or in A_{215} extinction coefficients.]

In the second approach, we stopped an equivalent proteolysis reaction at 30 min and exposed the dissolved reaction

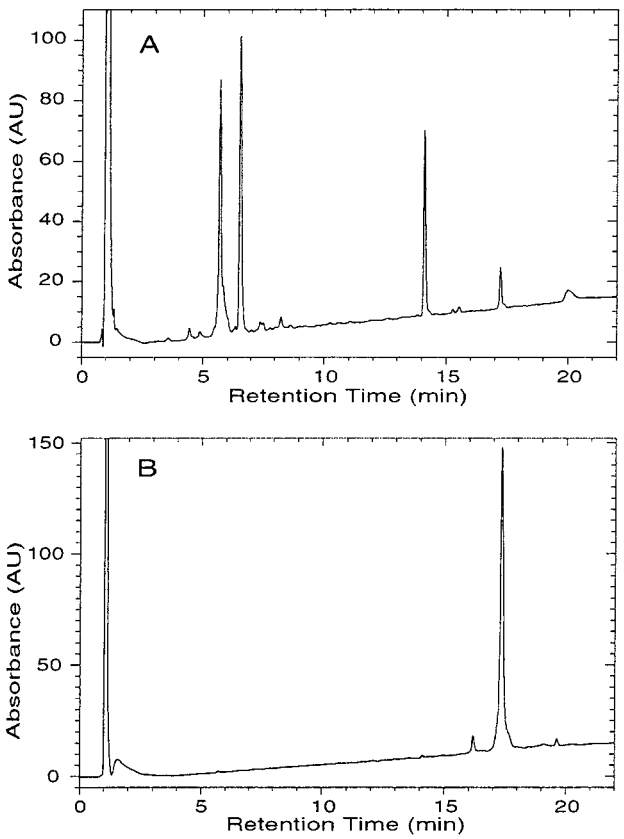

FIGURE 4: HPLC profiles of the (A) supernatant and (B) pellet after 30 min of tryptic digestion and 30 min of centrifugation to separate fibrils from the peptides released into the supernatant.

mixture to HPLC analysis. The single peak eluting at the normal elution positions of full-length Aβ(1−40) was collected. This material was subjected to N-terminal sequence analysis. Three tracks were obtained: the mature N-terminus (150 pmol), a sequence starting at position 6 (105 pmol), and a sequence starting at position 29 (30−45 pmol). [Note that the 6−40 and 29−40 fragments coelute with the 1−40 peptide in our HPLC system (Table 1).] Absolute determination of the amount of 1−5 peptide represented in the 1−40 peptide isolated from the trypsin digest of fibrils is difficult (due to highly variable yields in the Edman degradation chemistry and other factors), but it is clear from this analysis that a substantial portion (approximately 50% of the material in the proteolysis-resistant cores remaining at 30 min) of full-length Aβ(1−40) is still intact when 1−5 fragment release has reached a plateau, qualitatively supporting the results shown in Figure 3B.

Together, these experiments suggest that the incomplete release of 1−5 by trypsin shown in Figure 3B is not an artifact of 1−5 quantitation, but rather must be due to a portion of the Aβ(1−40) molecule being in a different environment within the fibril, an environment that protects the Arg_5−His_6 site from trypsin digestion.

The kinetics shown in Figure 3 were conducted on unfractionated aliquots of the trypsin digestion of fibrils. To learn about the physical status in the digest itself of these various fragments, we conducted an experiment in which a 30 min time point of a trypsin digest was centrifuged an additional 30 min. The supernatant and pellet were independently analyzed by HPLC. Figure 4A shows that essentially all of the 6−16, 1−5, and 17−28 fragments in the digest are found in the supernatant, along with a small amount of the 29−40 peptide. Figure 4B shows that the pellet contains a large peak corresponding to the coelution position of the 1−40, 6−40, and 29−40 peptides. Mass spectrometry (not shown) confirmed that this peak contains all three of these peptides. According to this analysis, only a portion of the total 29−40 peptide generated at 30 min remains with the fibril. It is not clear if this is because it is buried in an interior region of fibril structure or because its hydrophobic character favors continued noncovalent association with the fibril. It is also not possible to tell whether the small amount of cleavage at the 28−29 bond to generate the 17−28 and 29−40 fragments occurred as an initial hit on fibril-incorporated 1−40, 6−40, or 17−40 or on soluble peptides after they are released from the fibrils. (However, as discussed above, the most likely source is from proteolytic cleavage of peptides released from the fibril.)

The makeup of the insoluble portion of this partial digest is also significant for what is *not* present. The absence of detectable amounts of the 17−40 peptide associated with the fibrils suggests that the Lys_{16}−Leu_{17} bond is not available when Aβ(1−40) is incorporated within the fibril (compare to the presence of the 11−40 fragment in the pellet of a partial chymotrypsin reaction, as described below).

In summary, the trypsin reaction rapidly releases the 1−5 fragment until a plateau at about 80% of the maximum possible yield of 1−5 is reached, after which no further digestion occurs. This suggests two environments for the N-terminus of Aβ(1−40) in fibrils: one in which the peptide is as exposed to trypsin cleavage as it is in the monomeric peptide and one in which it is strongly protected from trypsin cleavage. It is important to note that protection within the core structure of trypsin-resistant Aβ fibrils is only feasible to the extent that this core is stable; this is relevant since, as discussed below, it appears that no such highly stable core exists in the chymotrypsin digest of fibrils.

Chymotrypsin Reactions. The eight panels of Figure 5 show the kinetics by which some peptide fragments are released from the Aβ(1−40) monomer and fibrils by chymotrypsin digestion at pH 7.9 and 25 °C. The data are shown as mole fractions computed using the $\mu g/A_{215}$ conversion factor for HPLC peak areas derived from full-length Aβ-(1−40). Since, as shown in Figure 2, most elements of the Aβ sequence are represented in multiple chymotrypsin digestion fragments, it was not feasible to normalize the proteolysis kinetics data as was done for the trypsin reaction.

One peptide, the 1−4 fragment, stands out as being released from fibrils as rapidly as from monomer (Figure 5A). While this fragment is generated from fibrils to a mole fraction of about 0.5 within the first 10 min, other fragments are generated to a mole fraction of less than 0.1 in the same time frame. As with the trypsin reactions, the mechanism by which these other fragments are released from fibrils is not clear, and no conclusions can be drawn about the possible availability of the corresponding cleavage sites within fibrils. The 4−5 bond, however, appears to be as available for chymotrypsin cleavage within the fibril as within the monomer, consistent with the trypsin results. Also consistent with the trypsin results, the 1−4 release curve appears to engage a slower kinetic phase at a value of about mole fraction 0.80 after about 40−60 min. This value must be viewed as approximate, since the chymotrypsin digest of

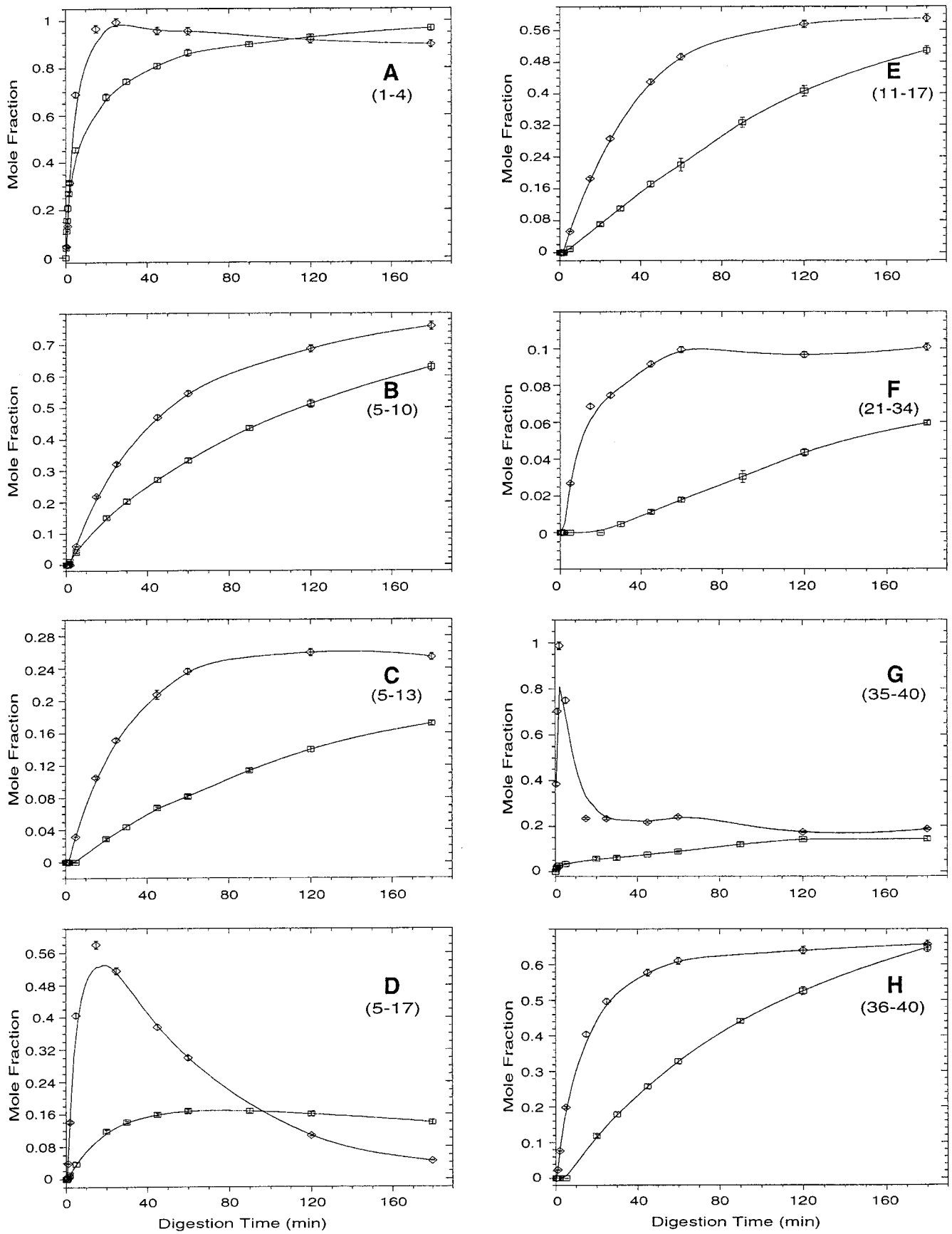

FIGURE 5: Mole fraction of peptides released after digestion using chymotrypsin vs time from the monomer (◇) and fibrils (□). The data points have been connected using smooth curves.

fibrils is somewhat more aggressive than it is for trypsin, proceeding almost to completion and therefore not defining a clear plateau level.

It is interesting to compare the progress curve of generation of the 36−40 fragment to that of the 1−4 fragment. These peptides are derived from opposing ends of Aβ(1−40). They

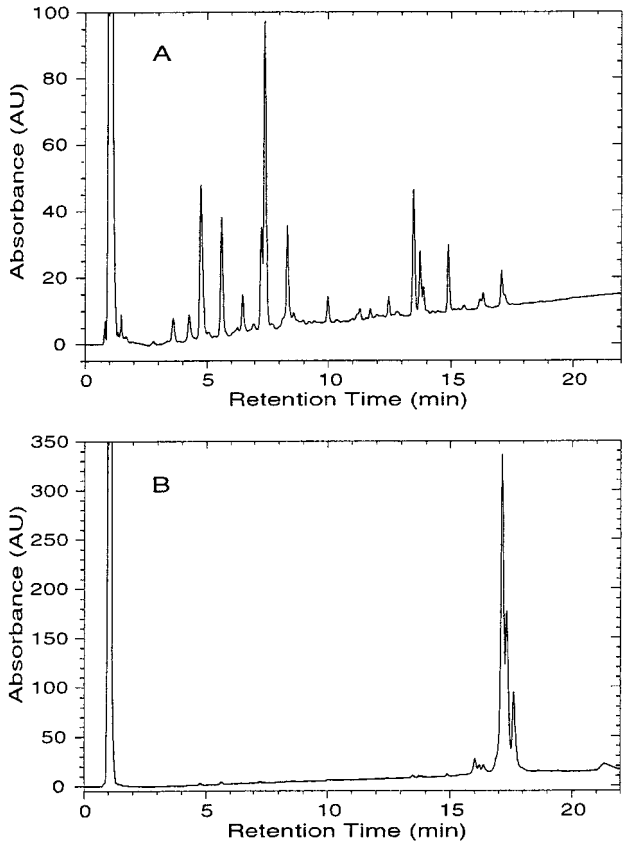

FIGURE 6: HPLC profiles of the (A) supernatant and (B) pellet after 15 min of digestion using chymotrypsin and 30 min of centrifugation to separate fibrils from the peptides released into the supernatant.

are released with similar kinetics from the monomer, with the reaction reaching completion within the first 20 min of the digests. However, the peptides are released from fibrils with quite different kinetics. The data suggest that the 35−36 peptide bond is protected from access by chymotrypsin within the fibril structure.

In contrast to the well-ordered kinetics of release of the 36−40 fragment, the progress curve of the 35−40 fragment release from the monomer contains an aberration, in that it proceeds with a burst of material within the first few minutes and then decays to its final level by 20 min. This cannot be explained by its being an intermediate, since no smaller peptides derived from the 35−40 fragment are observed in the digest and since the 35−40 peak would be expected to decay to zero if it were truly an intermediate. Rather, we think it reflects the appearance and disappearance of another, unidentified, proteolysis intermediate that coelutes with the 35−40 peptide. No attempt was made to isolate and identify this transient species.

Figure 6 shows the chromatograms obtained for the supernatant and pellet of an aliquot taken from the chymotrypsin digest after 15 min and centrifuged at 14 000 rpm and 25 °C for 30 min. The results are very similar to the corresponding experiment for the trypsin digest (Figure 4). Most of the peptide fragments are found in the supernatant. The pellet contains only very long fragments possessing an intact C-terminus. (In contrast to the trypsin digest, the peptide components of the insoluble material are separable in our HPLC system.) The presence of intact Aβ(1−40) confirms the presence of a significant fraction of Aβ possessing a Phe_4−Arg_5 bond that is protected from chymotrypsin hydrolysis. We interpret the presence of a relatively small amount of the 11−40 fragment as an indication of the availability to chymotrypsin binding and cleavage of the Tyr_{10}−Glu_{11} bond within the fibril structure. An alternative explanation is that it stems from chymotrypsin cleavage of Aβ(1−40) that has dissociated from the fibril, after which the 11−40 fragment reassociates with the fibril. This seems very unlikely, however, since we would expect that the 11−40 fragment would be very quickly further digested if it were free in solution. (Furthermore, if such a chain of events were possible, one would also expect a significant amount of the 17−40 fragment to accumulate in the trypsin digest of Aβ fibrils, which does not occur.) Thus, the best interpretation is that the Tyr_{10}-Glu_{11} bond is available within the fibril structure, but not to the extent of the Phe_4−Arg_5 bond (compare panels A, B, and C of Figure 5). If the Tyr_{10}−Glu_{11} bond can be cleaved in Aβ molecules residing within fibril structure, this implies that approximately the first 15 residues of the Aβ(1−40) molecule are not fixed in stable, protective structure within the fibril.

DISCUSSION

Limited proteolysis has been used to map surface-exposed, flexible, or weakly structured areas of folded, globular, monomeric, and oligomeric proteins (*6*, *8*) and to assess protein folding dynamics (*7*). The basic premise of the method is that cleavage requires both the existence of an appropriate protease recognition sequence in the protein of interest and the availability of that sequence for cleavage. The latter generally requires that the cleavage site exist at the center of a 4−10 residue segment in a flexible conformation that can bind and adapt to the protease active site (*8*). The observation of an especially rapid cleavage event in limited proteolysis means that that sequence element cleaved is either in an exposed, extended conformation in the native, folded state or that it transiently occupies such a state during the normal structural fluctuations of the protein under the experimental conditions. In a typical limited proteolysis experiment, conditions are adjusted to restrict proteolysis, if possible, to a single cleavage event; the site of this cleavage event is then identified. In the experiments described here, we took advantage of the fact that the Aβ monomer exists in an unstructured, random coil state under native conditions (*14*). This allowed us to measure actual rates of proteolytic generation of fragments from the monomeric peptide and to compare these data to fragment generation rates from the Aβ fibril.

The studies described here generated two major results. First, both the trypsin and chymotrypsin digestion experiments showed a rapid release of an N-terminal fragment of Aβ, due to cleavage either at the Arg_5−His_6 bond (trypsin) or the Phe_4−Arg_5 bond (chymotrypsin). These N-terminal peptides are released from fibrils at about the same rate as they are released during digestion of the monomer, suggesting that the steric accessibility of the peptide regions surrounding the corresponding cleavage sites must not be appreciably altered when these peptides are built into fibrils. Evidence from analysis of the pellet fraction of partial digests also suggests that the Tyr_{10}−Glu_{11} bond is accessible within the fibrils, while the Lys_{16}−Leu_{17} bond is not.

Although the rapid cleavage of the Phe_4-Arg_5 and Arg_5-His_6 bonds, and the slower but significant cleavage at the $Tyr_{10}-Glu_{11}$ bond, strongly suggests that these bonds are in flexible segments of Aβ within the fibril structure, it is not possible to say exactly how far this flexible or weak structure might extend beyond the $Tyr_{10}-Glu_{11}$ bond toward the C-terminus. Conservatively, two residues on either side of a cleavage site are required by most proteases for strong binding and cleavage (*8*). However, modeling studies also show that potential sites must be located in a flexible segment 10−12 residues long before that segment can conform to the rigid conformational requirements of the protease for binding (*8*, *15*). This suggests that the Aβ sequence extends to somewhere between residue 13 and 16 before encountering the stable structure in the fibril. Since cleavage of the $Lys_{16}-Leu_{17}$ bond is not detectable, it is likely that this flexible structure does not extend beyond residue 16.

Hydrogen−deuterium exchange experiments suggest that only about 50% of the backbone amides of the Aβ(1−40) peptide exist in the protective H-bonded structure in the amyloid fibril (*5*), implying that about half of the 39 backbone amides are not in the H-bonded secondary structure. The limited proteolysis experiments described here suggest that about 13−16 of these non-H-bonded, unprotected amide groups must exist in the N-terminus of the peptide. This is not surprising, since the N-terminus of Aβ is relatively hydrophilic (see Figure 2), deriving from the extracellular portion of the APP molecule, while the C-terminal part of Aβ is highly hydrophobic, deriving from the transmembrane domain of APP (*16*). The existence of the more hydrophobic part of Aβ in the β-sheet structure might have been predicted, in analogy with the strong hydrophobic contribution seen in the packing of β-sheets of β-sandwich proteins (*17*) and the hydrophobic character of many amyloidogenic peptides. However, some hydrophilic sequences also are capable of forming amyloid or amyloid-like aggregates, including the aggregation domains of yeast prions (*18*) and the polyglutamine sequences associated with expanded CAG repeat diseases such as Huntington's disease (*19*). Our results show that, at least in the case of Aβ, the hydrophilic portion of the peptide sequence in not intimately involved in the amyloid β-sheet structure.

The location of the additional non-H-bonded structure in the Aβ peptide predicted by the hydrogen−deuterium exchange analysis cannot be deduced from our limited proteolysis data. One possibility for this additional non-H-bonded segment would be a β-turn or small loop somewhere within the β-sheet-rich C-terminal region of Aβ. Since a tight turn or small loop would not be expected to be protected from H-exchange, it might be expected that three to five exchangeable backbone amide hydrogens might derive from such a structure. At the same time, since 10−12 residues in flexible conformation are required for proteolytic cleavage (*8*, *15*, *20*), it is unlikely that a tight turn or short loop would be cleaved in a limited proteolysis experiment, even if they possessed an appropriate primary cleavage site. As discussed in the Results section, we do not consider the existence of a small amount of the 29−40 fragment in the fibril fraction of the partial trypsin digest to be compelling evidence for the accessibility of the $Lys_{28}-Gly_{29}$ bond within the intact fibril. Thus, the existence and location of a chain reversal element in the Aβ fibril cannot be addressed by our limited proteolysis results. Ongoing studies, such as more detailed hydrogen-exchange experiments, should pinpoint any additional elements of sequence not involved in the β-sheet.

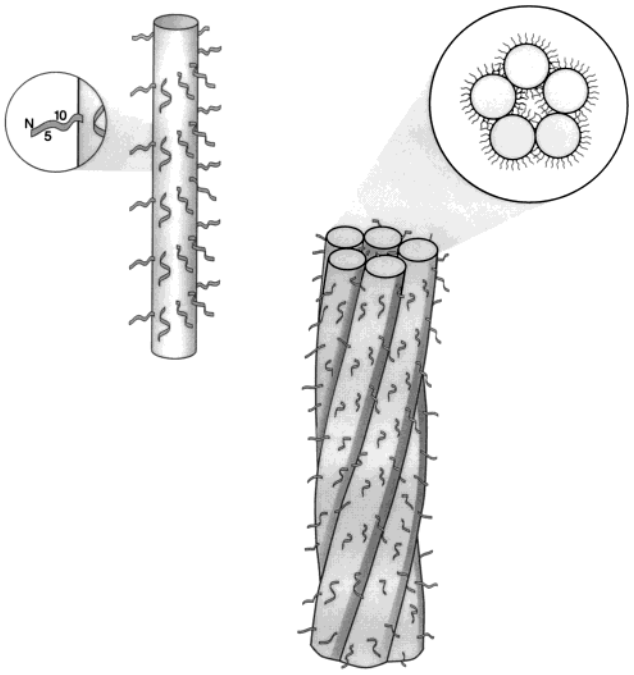

FIGURE 7: Model for the Aβ fibril structure consistent with the data described in this paper. The upper left part of the figure shows a model for a protofilament component of the amyloid fibril from which the N-terminal segments of the Aβ peptide project at regular intervals. As discussed in the text, N-terminal residues up to a point somewhere in the region 12−16 appear to be exposed to proteolysis in the fibril structure. The lower right portion of the figure shows the bundling of five such protofilaments into a fibril, as suggested by X-ray diffraction analysis of Aβ fibrils (*22*). The highlighted end view of this fibril model shows how bundling of protofilaments would be expected to protect a portion of the projecting Aβ N-termini from a large structural probe such as a protease. The model shown here is meant to illustrate how protofilament bundling creates a protected subpopulation of protruding Aβ N-termini. Other details of the model, such as the pitch of the Aβ termini emerging from the protofilament and the pitch of the protofilaments within the fibril, are for illustrative purposes only.

The second major result of this work is the discovery that Aβ exists in two distinct environments within the fibril. The major portion of fibrillar Aβ has an exposed N-terminus, as described above. There is also a significant minor portion, however, in which the N-terminus is protected from proteolysis. This result is especially clear in the trypsin experiments, where the proteolytic release of the 1−5 peptide plateaus at about 80% of the theoretical yield of 1−5. The chymotrypsin results suggest a similar distribution between exposed and protected N-termini.

One explanation for the existence of two environments for the N-terminus is illustrated schematically in Figure 7. Amyloid fibrils are bundles of smaller units, called protofilaments, that laterally associate to form the twisted fibril structure seen in electron and atomic force micrographs (*12*, *21*). The number of protofilaments per fibril varies among the different amyloids, with Aβ fibrils estimated to consist of three to five bundled filaments based on X-ray diffraction data (*22*). Figure 7 shows one way in which such an Aβ amyloid fibril might be constructed. If, as suggested by the results described here, the N-terminus of Aβ is excluded from

the β-sheet network of the fibril, it would be expected to project out into solution from the protofilament core. However, Figure 7 suggests that a certain percentage of the Aβ N-termini projecting from protofilament surfaces will be sequestered between protofilaments in the core or lumen of the fibril. These buried termini might be expected to be protected from proteolysis so long as the fundamental bundled protofilament structure remains intact. The geometry of the protofilament packing in this model suggests that about 25% of the N-termini might be so buried, which would be consistent with the proteolysis data. The presence of the Aβ N-terminus at protofilament packing junctions suggests a role for the N-terminus in stabilizing the fibril by facilitating protofilament interactions.

Our results are consistent with a number of previous structure−function studies on Aβ fibril formation and structure. Our observation that the N-terminal 13−16 residues of Aβ are exposed on the fibril surface in the flexible or weak structure—which may, nonetheless, be important for protofilament interactions—is consistent with the previous observation (from fragment studies) that His_{13} and His_{14} may play an important role in stabilizing protofilament packing (*23*). Our result suggesting that the Aβ sequence approximately after residue 16 is involved in stable structure in the fibril is consistent with the previously documented importance of the C-terminal residues in fibril formation (*24*) and with the importance of residues 16−20 in packed (*25*) and/or β-sheet (*26*, *27*) residues as implied by amino acid substitution experiments and by peptide inhibitor studies (*28*−*31*).

Since several models have been proposed for the protofilament folding motif of amyloid fibrils (*4*, *32*−*35*), one can consider how readily the Aβ sequence "threads" into the folding motif of a particular model. Our data are consistent with any model that allows for the majority of the N-termini of the Aβ sequence to be excluded from the β-sheet network of the protofilament as protease-sensitive elements. Experimental data from limited proteolysis, hydrogen−deuterium exchange, and other techniques will be important in the future for testing and refining models of fibril structure.

Significantly, our in vitro studies of Aβ fibril proteolytic susceptibility are also consistent with analysis of Aβ peptides isolated from amyloid plaques of Alzheimer's disease patients, which reveals significant N-terminal heterogeneity (*36*). Although formally it has not been possible to determine, in AD or in other amyloid diseases, whether proteolysis in vivo occurs before or after fibril formation, our results are entirely consistent with the hypothesis that proteolytic fragmentation occurs after amyloid fibril formation in Aβ amyloid plaques in the AD brain.

Our ability to obtain interpretable kinetic data in the limited proteolysis of amyloid fibrils is somewhat surprising, given the expectation that fibril clumping and settling, combined with slow diffusion rates, might compromise efficient mixing and restrict protease−substrate collisions. The observation of initial cleavage rates at sites within the N-terminal region of Aβ that are essentially identical for fibril and the monomer is especially interesting in this context. This result suggests that the diffusion limit on collisions between protease and protein substrate is not significantly altered when the substrate is a large protein aggregate and implies that limited proteolysis may prove to be a valuable technique for studying the structures of other protein aggregates.

The success of the limited proteolysis approach in analyzing fibril structure suggests that other classical methods for protein analysis, such as chemical modification (*37*), may also prove useful in attacking the important contemporary problem of amyloid fibril structure. For example, we recently found that a Cys residue substituted for Phe_{19} in Aβ(1−40) is fully protected from alkylation with iodoacetate when the peptide is incorporated into fibrils (A. Williams and R. Wetzel, unpublished results). This result is consistent with the involvement of the side chain of residue 19 in the buried structure within the fibril, consistent with the limited proteolysis data described here.

ACKNOWLEDGMENT

We acknowledge Hart Graphics, Knoxville, TN, for preparation of Figure 7.

REFERENCES

1. Sipe, J. D. (1992) *Annu. Rev. Biochem. 61*, 947−975.
2. Falk, R. H., Comenzo, R. L., and Skinner, M. (1997) *N. Engl. J. Med. 337*, 898−909.
3. Martin, J. B. (1999) *N. Engl. J. Med. 340*, 1970−1980.
4. Sunde, M., Serpell, L. C., Bartlam, M., Fraser, P. E., Pepys, M. B., and Blake, C. C. (1997) *J. Mol. Biol. 273*, 729−739.
5. Kheterpal, I., Zhou, S., Cook, K. D., and Wetzel, R. (2000) *Proc. Natl. Acad. Sci. U.S.A. 97*, 13597−13601.
6. Neurath, H. (1980) in *Protein Folding* (Jaenicke, R., Ed.) pp 501−523, Elsevier, Amsterdam.
7. Fontana, A., Polverino de Laureto, P., De Filippis, V., Scaramella, E., and Zambonin, M. (1997) *Fold. Des. 2*, R17−R26.
8. Hubbard, S. J. (1998) *Biochim. Biophys. Acta 1382*, 191−206.
9. Zagorski, M. G., Yang, J., Shao, H., Ma, K., Zeng, H., and Hong, A. (1999) *Methods Enzymol. 309*, 189−204.
10. LeVine, H. (1999) *Methods Enzymol. 309*, 274−284.
11. Wood, S. J., Maleeff, B., Hart, T., and Wetzel, R. (1996) *J. Mol. Biol. 256*, 870−877.
12. Nybo, M., Svehag, S.-E., and Nielsen, E. H. (1999) *Scand. J. Immunol. 49*, 219−223.
13. Harper, J. D., and Lansbury, P. T., Jr. (1997) *Annu. Rev. Biochem. 66*, 385−407.
14. Gursky, O., and Aleshkov, S. (2000) *Biochim. Biophys. Acta 1476*, 93−102.
15. Hubbard, S. J., Eisenmenger, F., and Thornton, J. M. (1994) *Protein Sci. 3*, 757−768.
16. Selkoe, D. J. (1994) *Annu. Rev. Neurosci. 17*, 489−517.
17. Cohen, F. E., Sternberg, M. J., and Taylor, W. R. (1981) *J. Mol. Biol. 148*, 253−272.
18. Glover, J. R., Kowal, A. S., Schirmer, E. C., Patino, M. M., Liu, J. J., and Lindquist, S. (1997) *Cell 89*, 811−819.
19. Scherzinger, E., Sittler, A., Schweiger, K., Heiser, V., Lurz, R., Hasenbank, R., Bates, G. P., Lehrach, H., and Wanker, E. E. (1999) *Proc. Natl. Acad. Sci. U.S.A. 96*, 4604−4609.
20. Hubbard, S. J., Beynon, R. J., and Thornton, J. M. (1998) *Protein Eng. 11*, 349−359.
21. Harper, J. D., Lieber, C. M., and Lansbury, P. T., Jr. (1997) *Chem. Biol. 4*, 951−959.
22. Malinchik, S. B., Inouye, H., Szumowski, K. E., and Kirschner, D. A. (1998) *Biophys. J. 74*, 537−545.
23. Fraser, P. E., McLachlan, D. R., Surewicz, W. K., Mizzen, C. A., Snow, A. D., Nguyen, J. T., and Kirschner, D. A. (1994) *J. Mol. Biol. 244*, 64−73.
24. Halverson, K., Fraser, P. E., Kirschner, D. A., and Lansbury, P. T. J. (1990) *Biochemistry 29*, 2639−2644.

25. Hilbich, C., Kisters-Woike, B., Reed, J., Masters, C. L., and Beyreuther, K. (1992) *J. Mol. Biol. 228*, 460−473.
26. Wood, S. J., Wetzel, R., Martin, J. D., and Hurle, M. R. (1995) *Biochemistry 34*, 724−730.
27. Teplow, D. B., Lomakin, A., Benedek, G. B., Kirschner, D. A., and Walsh, D. M. (1997) in *Alzheimer's Disease: Biology, Diagnosis and Therapeutics* (Iqbal, K., Winblad, B., Nishimura, T., Takeda, M., and Wisniewski, H. M., Eds.) pp 313−321, Wiley, New York.
28. Tjernberg, L. O., Naslund, J., Lindqvist, F., Johansson, J., Karlstrom, A. R., Thyberg, J., Terenius, L., and Nordstedt, C. (1996) *J. Biol. Chem. 271*, 8545−8548.
29. Ghanta, J., Shen, C. L., Kiessling, L. L., and Murphy, R. M. (1996) *J. Biol. Chem. 271*, 29525−29528.
30. Soto, C., Kindy, M. S., Baumann, M., and Frangione, B. (1996) *Biochem. Biophys. Res. Commun. 226*, 672−680.
31. Findeis, M. A., Musso, G. M., Arico-Muendel, C. C., Benjamin, H. W., Hundal, A. M., Lee, J. J., Chin, J., Kelley, M., Wakefield, J., Hayward, N. J., and Molineaux, S. M. (1999) *Biochemistry 38*, 6791−6800.
32. Inouye, H., Fraser, P. E., and Kirschner, D. A. (1993) *Biophys. J. 64*, 502−519.
33. Chaney, M. O., Webster, S. D., Kuo, Y. M., and Roher, A. E. (1998) *Protein Eng. 11*, 761−767.
34. Lazo, N. D., and Downing, D. T. (1998) *Biochemistry 37*, 1731−1735.
35. Tjernberg, L. O., Callaway, D. J., Tjernberg, A., Hahne, S., Lilliehook, C., Terenius, L., Thyberg, J., and Nordstedt, C. (1999) *J. Biol. Chem. 274*, 12619−12625.
36. Roher, A. E., Lowenson, J. D., Clarke, S., Wolkow, C., Wang, R., Cotter, R. J., Reardon, I. M., Zurcher-Neely, H. A., Heinrikson, R. L., Ball, M. J., et al. (1993) *J. Biol. Chem. 268*, 3072−3083.
37. Means, G. E., and Feeney, R. E. (1971) *Chemical Modification of Proteins*, Holden-Day, San Francisco.

BI010805Z